Disentanglement Time of Polymers Determines the Onset of Rim Instabilities in Dewetting

Sylvain Gabriele,[1,2] Séverine Sclavons,[2] Günter Reiter,[3] and Pascal Damman[2,*]
[1]Laboratoire de Physicochimie des Polymères, Materia Nova asbl, Parc Initialis, 1, Avenue N. Copernic, B-7000 Mons, Belgium
[2]Laboratoire de Physicochimie des Polymères, Université de Mons Hainaut, 20, Place du Parc, B-7000 Mons, Belgium
[3]Institut de Chimie des Surfaces et Interfaces, CNRS, 15, rue Jean Starcky, Boîte Postale 2488, 68057 Mulhouse Cedex, France

(Received 30 September 2005; revised manuscript received 8 March 2006; published 21 April 2006)

Molecular relaxations determine the viscoelastic properties of polymers, which, in turn, control macroscopic processes like dewetting. Here, we demonstrate experimentally that the onset of rim instabilities is correlated with the longest relaxation (''reptation'') time of the dewetting polymer. Conversely, such experiments allow us to determine the reptation time of polystyrene in thin films as a function of molecular weight. Our approach opens up new possibilities for testing rheological properties of polymers confined in thin films.

DOI: 10.1103/PhysRevLett.96.156105 PACS numbers: 68.60.−p, 61.41.+e, 68.15.+e, 83.50.−v

Since the successful introduction of the reptation model by de Gennes [1] and Doi-Edwards [2–5], which describes how chainlike polymers move in a melt of identical chains, considerable effort has been directed to improve the original model. Several major theoretical refinements such as tube length fluctuations [6] or convective constraint release [7] were proposed. In systems like thin films, chain movement may be affected by confinement. Thus, we have to experimentally probe and to understand polymer relaxation mechanisms in thin films. However, in spite of the great relevance of direct measurements of the longest relaxation times, i.e., reptation (disentanglement) times, there are only a few such measurements of disentanglement times in thin films. The time dependence of interdiffusion of long polymer chains was previously studied by neutron reflectivity [8–11] and more recently, Richter and coworkers estimated the reptation time of polymeric systems by neutron spin-echo spectroscopy measurements [12]. In addition, relaxation dynamics of end-to-end vectors (normal modes) in ultrathin films, much thinner than the unperturbed dimension of polymer chains, were also investigated by dielectric spectroscopy [13,14]. Recently, Dutcher and coworkers have shown that microscopic measurements of hole growth in freely standing polystyrene films allow us to observe a shear deformation and therefore provide a possible test case for the tube theory of entangled polymer dynamics [15].

In this Letter, we report a novel concept, also based on microscopy measurements, which allows us to extract reptation times from the rim instability for nanoscale polymer films dewetting at temperatures close to the glass transition. We will demonstrate that, and explain why, the onset time of such rim instabilities, occurring at the transition between two dewetting regimes, is related to the reptation time.

On nonwettable substrates and for thicknesses lower than the critical thickness (h_c) determined by gravity, polymer thin films are not stable and will eventually dewet. Dewetting starts after the formation of a three-phase contact line where substrate, film, and environment (e.g., air) meet. The dynamics of the movement of this contact line is determined by the balance of capillary driving forces (action) and dissipation (reaction of the moving part) into the rim collecting the dewetted fluid. One or more dissipation mechanisms may be at work depending on the substrate-fluid interaction and the nature of the fluid. On slippery substrates [16,17] and for polymer melts such as polydimethylsiloxane (PDMS), which at the time scale of the experiment are purely viscous (i.e., with very short disentanglement times), Reiter and Sharma reported [18] that dewetting of polymers leads systematically to shape fluctuations of the rim (variations in height and width) and subsequent fingering instabilities. The whole process is governed by a minimization of the surface energy and driven by Laplace pressure.

For the experiments presented here, we used thin polystyrene (PS) films spin-coated from toluene solution onto silicon wafers coated with a nonwettable PDMS thin layer. The length of the polymer varied as expressed by the molecular weights, M_w: 035, 50, 110, 233, 390, and 600 kg/mol. Polymers were supplied by Polymer Source and have polydispersity index I_p (as defined by the ratio of the weight average and number average molecular weight) of less than 1.1. Film thicknesses ranged from 50 to 100 nm, as measured by ellipsometry. We followed the dewetting of a straight line from the edge of the sample as a function of time with a CCD camera. The resulting micrographs have been analyzed with the IMAGEJ software [19].

Dewetting of viscoelastic materials on slippery substrates is controlled by dissipation of the capillary energy within the polymer film and via friction between the polymer chains and the substrate surface. We have shown previously that the shape of the rim allows us to clearly distinguish between two dewetting regimes. These dissipation regimes are also separated by a transition in the time dependence of the dewetting velocity occurring at a char-

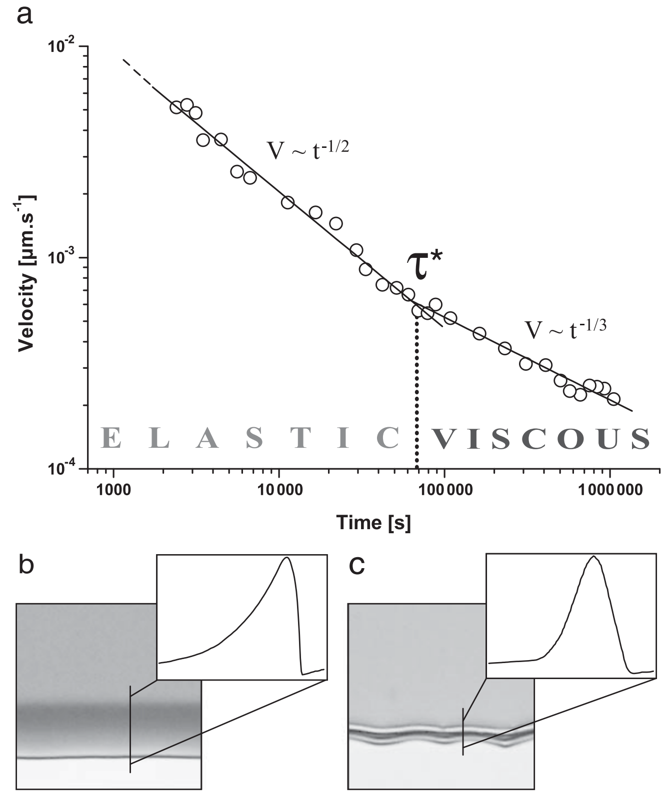

FIG. 1. (a) Dewetting dynamics of a polystyrene film ($M_w = 110$ K, $h_0 = 60$ nm, $T = 120$ °C) together with the corresponding dissipation mode. The dashed line in the logarithmic plot V versus t represent the characteristic time τ^*. Typical optical micrographs (45×45 μm^2, the thickness dependent contrast is based on interference of light reflected at the film and the substrate interface) and corresponding atomic force microscopy profiles of (b) a stable asymmetric rim ($M_w = 110$ kg/mol, $h_0 = 75$ nm, $T = 120$ °C) in the elasticity dominated regime and (c) an undulating rim shortly after τ^* ($M_w = 50$ kg/mol, $h_0 = 100$ nm, $T = 125$ °C).

acteristic time τ^* [20]. As shown in Fig. 1(a), τ^* corresponds to the transition from the elasticity dominated regime to a viscosity dominated regime.

For $t < \tau^*$, dewetting is highly affected by elastic behavior of the polymer, leading to the formation of asymmetric rims [Fig. 1(b)], with a steep side at the three-phase contact line and an exponential decay toward the film [21,22], as can be deduced from the interference contrast (succession from light brown to dark blue, for example). Asymmetric rims are found to be highly stable against transversal fluctuations [Fig. 1(b)]. This result is consistent with the fact that Laplace pressure is not equilibrated within the rim as clearly demonstrated by its asymmetric shape. Thus, transversal flows within the rim as observed in purely viscous systems like PDMS are not expected as long as the elastic behavior dominates. At τ^*, the systems enters the viscous dissipation dominated regime where the Laplace pressure within the rim can be minimized. The resulting constant Laplace pressure leads to a more symmetric rim shape which is a necessary condition to observe the transversal undulations in the rim [Fig. 1(c)]. For $t > \tau^*$, in the mature regime, the dewetting velocity can be found by equating the friction force, $F_f = (\eta/b)wV$, to the capillary force, $F_s = |S|$ which yields the following relation:

$$V = \frac{|S|b}{\eta} w^{-1}$$

where V, S, b, η, and w are the dewetting velocity, the spreading coefficient, the slippage length, the polymer melt viscosity, and the width of the rim, respectively. Solving this time-dependent equation, taking into account the mass conservation, gives the well-known relation $V \sim t^{-1/3}$ [23] which is consistent with our experiments [see Fig. 1(a)].

In contrast to previous studies of Plateau-Rayleigh instabilities of static liquid threads [24,25], we are dealing with a *moving* contact line. Moreover, the theory of the Plateau-Rayleigh instability was constructed for a the deformation of a ridge bound by two coupled contact lines. It leads to a characteristic wavelength which is proportional to the width of the ridge. However, for moving rims in the case of dewetting, there is only one three-phase contact line, denoted as the front side. As can be seen in Fig. 1(c) or in the insets of Fig. 2, the deformation of the three-phase contact line drives the instability whereas the other side of the rim, denoted as the rear side, is in contact with the film and stays stable. Another difference to static ridges is that,

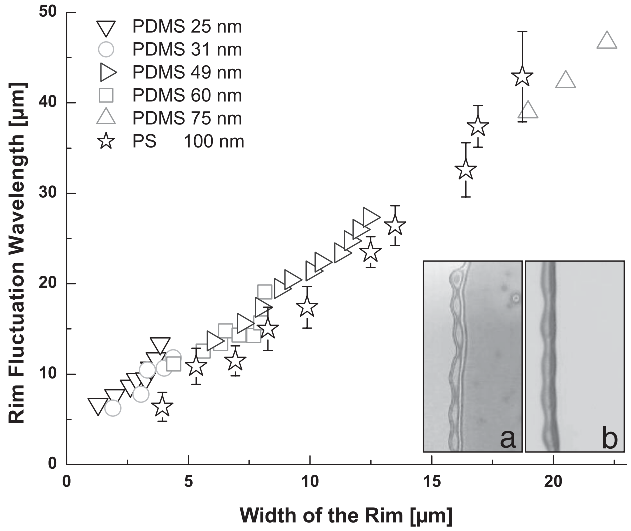

FIG. 2. Dependence of the average wavelength (λ_{exp}) of the rim undulations on the width (w) of the rim for PDMS thin films ($M_w = 308$ kg/mol, 25 nm $< h_0 <$ 75 nm) on PDMS-grafted substrates [26] and for a PS thin film ($M_w = 50$ kg/mol, $h_0 = 100$ nm) on an adsorbed PDMS substrate. The insets show typical optical micrographs of the undulating edge taken during the dewetting experiment of (a) PDMS films on grafted PDMS substrates [26] and (b) a PS film on an adsorbed PDMS substrate.

in the course of dewetting, the rim continuously grows by fluid accumulation. Because of the continuous increase of the rim width, the wavelength λ_{exp} characterizing the undulation of the deformed contact line (before droplet formation) continuously increases in time but always remains proportional to the rim width (Fig. 2). We found $\lambda_{\mathrm{exp}} = (2.1 \pm 0.2)w$ during all the dewetting experiment. We want to point out that our experimental results are in excellent agreement with previous experiments using PDMS thin films on grafted PDMS substrates (see Fig. 2) [26]. Shown in the Fig. 2, the cumulative presentation of data obtained for different polymers and various film thicknesses illustrates the universal behavior of the instability. Moreover, the evolution law characterizing the instability ($\lambda_{\mathrm{exp}} = (2.1 \pm 0.2)w$) is also in agreement with the theoretical ratio of wavelength to width ($\lambda_{\mathrm{th}} = 2.5w$) of a contact line instability presented in Ref. [27] based on a numerical resolution of the Navier-Stokes equation in the lubrication approximation.

The rim instability only appears after passing from the elasticity dominated to the viscosity dominated dissipation regime of dewetting. Consequently, a characteristic time exists to equilibrate the Laplace pressure within the rim, which, in turn, allows to obtain a symmetric rim morphology, necessary for the rim instability. Therefore, we can use the onset of this instability for determining the time, τ^* which characterizes the transition between the two dewetting regimes. As shown before, the wavy shape of the unstable rim, and consequently its contour length at the contact line, increases as dewetting proceeds. In order to obtain τ^*, we have measured this contour length as a function of time for different polystyrene molecular weights. The initial contour length of the straight and stable rim, l_0, is determined at the beginning of the dewetting experiment, before the onset of any transversal fluctuation. The formation of bulges and subsequent fingers increases the length of the three-phase contact line. As shown in Fig. 3, the dynamics of the instability is strongly dependent on the molecular weight, which is in agreement with the expression of the characteristic velocity of the liquid expressed by $V^* = \gamma/\eta$ [17] using γ, the surface tension, and η, the viscosity. The evolution of the contour length, represented via the ratio $l(t)/l_0$ as a function of the dewetting time, follows an exponential behavior described by the relation: $l(t)/l_0 = e^{\Delta t/A}$, where $\Delta t = t - \tau^*$ and A corresponds to the exponential rise time. This relation allows to determine via extrapolation on the semilogarithmic plot an onset-time where $l(t)/l_0$ starts to become larger than unity. Using such a procedure we were able to evaluate the onset time of undulations for different polystyrene molecular weights (see Fig. 3). Considering the large differences in dewetting dynamics with molecular weight (i.e., viscosity), we had to employ different temperatures for dewetting.

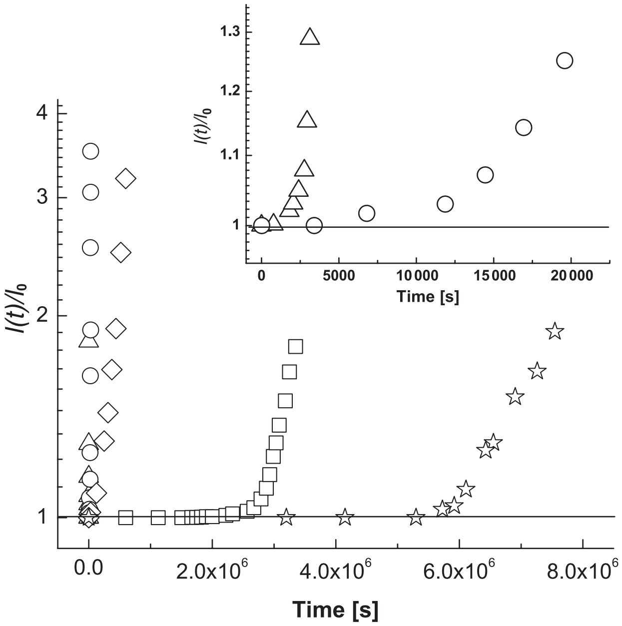

FIG. 3. Semilogarithmic plot of the temporal evolution of the normalized contour length $[l(t)/l_0]$ of the unstable three-phase contact line versus time (reduced to the reference temperature of 120 °C by the Williams-Landel-Ferry law [10]), measured for thin PS films of different molecular weights (M_w): 35 (triangles), 50 (circles), 233 (lozenges), 390 (squares), and 600 kg/mol (stars) and dewetted at 120, 125, 140, 145, and 150 °C, respectively. The inset shows $l(t)/l_0$ as a function of time for 35 (triangles) and 50 kg/mol (circles).

Figure 4 summarizes our results for τ^* and compares them with various experimentally determined values of the disentanglement time, τ_d. This comparison clearly and unambiguously shows that the characteristic time τ^* co-

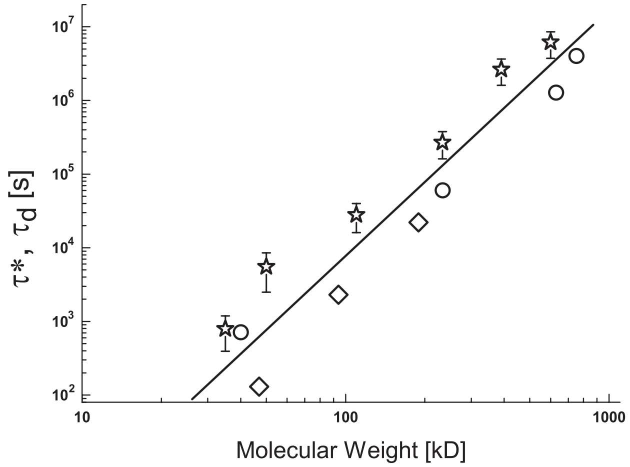

FIG. 4. Onset times of rim instabilities, τ^*, together with disentanglement times, τ_d, versus molecular weights. τ_d was obtained by neutron reflectivity (circles) and viscosity measurements (lozenges). The full line in the logarithmic plot of τ^*, τ_d versus molecular weights corresponds to the relation: $\tau_d \sim M^{3,4}$. The error bars reflect the variance of the repeated measurements.

incides well with disentanglement times obtained by neutron reflectivity [9–11] and viscosity measurements [28]. Therefore, we argue that determining the onset of rim instabilities represents a reliable way for measuring the longest relaxation time of a polymer melt. The measurements are simple and fast and can be performed under various conditions. This approach is ideally suited for testing theoretical predictions on relaxations in thin films for all fluids undergoing a transition from an elasticity to a viscosity dominated behavior as we have shown here for entangled linear polymers. Interestingly, our results suggest that the relation $\tau_d \sim M^{3,4}$ observed and theoretically predicted for bulk systems remains also valid for polymer thin films.

In summary, our results corroborate the assumption that a Plateau-Rayleigh instability is also at the origin of the undulation mechanism of a moving dewetting rim which eventually leads to a fingering instability. It became clear that this mechanism is only effective in a viscosity dominated regime of dewetting when Laplace pressure is determining the shape of the rim. Besides the study on the fundamental physics of why and how such instabilities develop, our most remarkable result concerns the use of the onset of this instability as an attractive experimental tool for observing relaxation processes in complex fluids and for determining the disentanglement time of nanometric polymeric films. This opens up new possibilities for testing polymer dynamics in confined geometries, maybe even for dimensions less than the size of the unperturbed polymer coil. We hope that our experimental results presented here will stimulate corresponding theoretical works.

We wish to thank Thomas Vilmin and Elie Raphaël for insightful discussions. We are grateful to Michel Voué for ellipsometry measurements and to Séverine Coppée and Roberto Lazzaroni for AFM measurements. Financial support from the European Social Fund (FSE) and the Belgian National Fund for Scientific Research (FNRS) is gratefully acknowledged. P. Damman is a Research Associate of the FNRS.

---

*Electronic address: pascal.damman@umh.ac.be

[1] P. G. de Gennes, J. Chem. Phys. **55**, 572 (1971).

[2] M. Doi and S. F. Edwards, J. Chem. Soc., Faraday Trans. 2 **74**, 1789 (1978).

[3] M. Doi and S. F. Edwards, J. Chem. Soc., Faraday Trans. 2 **74**, 1802 (1978).

[4] M. Doi and S. F. Edwards, J. Chem. Soc., Faraday Trans. 2 **74**, 1818 (1978).

[5] M. Doi and S. F. Edwards, J. Chem. Soc., Faraday Trans. 2 **75**, 38 (1979).

[6] S. T. Milner and T. C. B. McLeish, Phys. Rev. Lett. **81**, 725 (1998).

[7] G. Marrucci, J. Non-Newtonian Fluid Mech. **62**, 279 (1996).

[8] A. Karim, A. Mansour, G. P. Felcher, and T. P. Russell, Phys. Rev. B **42**, 6846 (1990).

[9] E. Sivaniah, M. Sferrazza, R. A. L. Jones, and D. G. Bucknall, Phys. Rev. E **59**, 885 (1999).

[10] G. Reiter and U. Steiner, J. Phys. II **1**, 659 (1991).

[11] D. G. Bucknall, S. A. Butler, and J. S. Higgins, Macromolecules **32**, 5453 (1999).

[12] P. Schleger, B. Farago, C. Lartigue, A. Kollmar, and D. Richter, Phys. Rev. Lett. **81**, 124 (1998).

[13] A. Serghei and F. Kremer, Phys. Rev. Lett. **91**, 165702 (2003).

[14] K. Fukao, Eur. Phys. J. E **12**, 119 (2003).

[15] C. B. Roth, B. Deh, B. G. Nickel, and J. R. Dutcher, Phys. Rev. E **72**, 021802 (2005).

[16] Long polymers on a nonadsorbing substrate have been found to slip and therefore the fluid velocity profile is not zero at the fluid-substrate interface [17]. The parameter b, called slippage length, characterizes the degree of "slipperiness" and corresponds to the distance behind interface at which the liquid velocity extrapolates to zero.

[17] C. Redon, J. B. Brzoska, and F. Brochard-Wyart, Macromolecules **27**, 468 (1994).

[18] G. Reiter and A. Sharma, Phys. Rev. Lett. **87**, 166103 (2001).

[19] W. Rasband, computer code IMAGEJ, http://rsb.info.nih.gov/ij.

[20] P. Damman, N. Baudelet, and G. Reiter, Phys. Rev. Lett. **91**, 216101 (2003).

[21] G. Reiter, M. Hamieh, P. Damman, S. Sclavons, S. Gabriele, T. Vilmin, and E. Raphaël, Nat. Mater. **4**, 754 (2005).

[22] G. Reiter, Phys. Rev. Lett. **87**, 186101 (2001).

[23] F. Brochard-Wyart, G. Debregeas, R. Fondecave, and P. Martin, Macromolecules **30**, 1211 (1997).

[24] K. Sekimoto, R. Oguma, and K. Kawasaki, Ann. Phys. (N.Y.) **176**, 359 (1987).

[25] F. Brochard-Wyart and C. Redon, Langmuir **8**, 2324 (1992).

[26] G. Reiter, J. Adhes. **81**, 381 (2005).

[27] A. Münch and B. Wagner, Physica (Amsterdam) **209D**, 178 (2005).

[28] D. J. Plazek and V. M. O'Rourke, J. Polym. Sci., Polym. Chem. **9**, 209 (1971).